IEEE Access
Multidisciplinary ⋮ Rapid Review ⋮ Open Access Journal

Received October 17, 2020, accepted October 31, 2020, date of publication November 9, 2020, date of current version November 19, 2020.

Digital Object Identifier 10.1109/ACCESS.2020.3036744

Multilayer Network Optimization for 5G & 6G

ALEJANDRO RAMÍREZ-ARROYO[1], PABLO H. ZAPATA-CANO[1], ÁNGEL PALOMARES-CABALLERO[1], JAVIER CARMONA-MURILLO[2], (Member, IEEE), FRANCISCO LUNA-VALERO[3], (Associate Member, IEEE), AND JUAN F. VALENZUELA-VALDÉS[1]

[1]Department of Signal Theory, Telematics and Communications, CITIC, Universidad de Granada, 18014 Granada, Spain
[2]Department of Computing and Telematics Engineering, Universidad de Extremadura, 06006 Badajoz, Spain
[3]Department of Languages and Computer Science, Universidad de Málaga, 29016 Málaga, Spain

Corresponding author: Alejandro Ramírez-Arroyo (alera@ugr.es)

This work was supported in part by the projects of the Spanish National Program of Research, Development, Innovation, under Grant TIN2016-75097-P, Grant RTI2018-102002-A-I00, and Grant EQC2018-004988-P, in part by the Junta de Andalucía under Project B-TIC-402-UGR18, in part by the European Regional Development Fund and Junta de Extremadura under Project IB18003, and in part by the Predoctoral Grant FPU19/01251 and Grant FPU18/01965.

ABSTRACT Mobile communications are growing and the number of users is constantly increasing at an accelerated rate, as well as the demand for the services they request. In the last few years, many efforts have focused on the design and deployment of the new fifth generation (5G) cellular networks. However, novel highly demanding applications, which are already emerging, need to go beyond 5G in order to meet the requirements in terms of network performance. But, at the same time, as the Earth does not allow us to increase the carbon footprint anymore, the energy consumption of the communication networks has to be critically taken into consideration. A multi-objective approach for addressing all these issues is therefore required. This work develops a cellular network framework that allows the evaluation of different system parameters over dynamic traffic patterns, as well as optimizing the different conflicting objectives simultaneously. The novelty relies on that the optimization process integrates key performance indicators from different layers of the network, namely the radio and the network layers, aiming at reaching solutions that account for the power consumption of the base stations, the total capacity provided to mobile users and also the signaling cost generated by handovers. Moreover, new metrics are needed to evaluate different solutions. Starting from the well-known energy efficiency merit factor (bits/Joule), three new merit factors are proposed to classify the network performance since they take into account several network parameters at the same time. These indicators show us the ideal working point that can be used to plan the point of operation of the network. These operation points are a medium-high power and capacity load and a low signaling load.

INDEX TERMS 5G networks, optimization, heterogeneous networks, energy efficiency.

I. INTRODUCTION

In 2019, the monthly mobile traffic reached 38 Exabytes, while this figure is estimated to be 160 Exabytes by 2025, at a 30 percent compound annual growth rate. On the other hand, the number of devices connected to the Internet will triple the world population by 2022, when there will be 3.6 devices per user compared to 2.4 devices per user in 2017 [1], [2]. This growth is due to the emergence of new applications on the Internet, such online video games, vehicular communications, tactile Internet, remote surgery, virtual reality (VR) and augmented reality (AR), which do not only require large bandwidths, but also challenging requirements such as a massive number of connections and ultra-low and reliable latency [3]–[5]. In order to meet these requirements, both public and private initiatives started to develop the new generation of mobile networks, the fifth or 5G, almost a decade ago. The design principles of this new technology were aimed at reaching 100x data rates, end-to-end delay below 1ms, 99.999% reliability, etc. Among them, given the current carbon footprint of the ICT industry [6], [7], these challenging operating requirements have to be achieved by saving 90% of the energy consumption. Three main target scenarios have been standardized in the Release 15 of

The associate editor coordinating the review of this manuscript and approving it for publication was Javed Iqbal.

the 3GPP consortium [8], namely, enhanced mobile broadband (eMBB), for providing the users with higher data rates than LTE, massive machine-type communications (mMTCs), for enabling a massive number of device connections, and, finally, ultra-reliable low-latency communications (uRLLC), aimed at low latency transmissions for small amounts of data with ultra-high reliability. Despite these predefined 5G scenarios, applications such as the tactile Internet does have requirements that go beyond 5G, as they need both extreme high data rates and ultra-reliable low latency. Therefore, the next generation networks (6G) will necessarily encompass new scenarios that combine the features of eMBB and uRLLC in order to provide services to the newly envisioned applications [9], [10].

Our working hypothesis is that a multi-layer optimization will be required to satisfy these demands, as it is proposed here. Indeed, this work targets these latter scenarios using a novel approach that jointly optimizes not only several performance criteria from both the radio and the network layer, but also considering energy efficiency issues [11]. From the radio interface, we have considered the capacity the network provides to the users, and the power consumption of the base stations (BSs). And, from the network layer, the number of bits used for signaling when a handover occurs due to the user mobility, as it is strongly correlated to the latency [12] required for uRLLC scenarios. To the best of our knowledge, these optimization objectives, which accounts for two complementary planes of the network, are yet rarely considered together. An accurate modeling of a heterogeneous network has been used, taking into consideration 5G enabling technologies [13] such as mmWave [14], massive MIMO [15], [16] and network densification [17].

The optimization of different layers of the network and energy at the same time is seldom reported in the literature. Several previous works related to the physical layer are, for example, the work of Zhang *et al.* [18]. They have proposed a joint power allocation, mode selection, and channel assignment scheme for optimizing energy efficiency in D2D (Device-to-Device) communications. Liu *et al.* [19] have performed two-dimensional optimization on traffic data rate and green energy generation on HetNets. Fletscher *et al.* [20], [21] have proposed several methods to optimize user allocation and energy efficiency simultaneously. Rengarajan *et al.* [22] and Di Renzo *et al.* [23] propose novelty models for the optimization of energy efficiency at the physical layer. On the other hand, works related to the network layer are, for example, the work of Keshavarzian *et al.* [24]. They have introduced several algorithms to minimize the energy consumption taking into account the mobility-aware capability. Muñoz *et al.* [25] optimize load balancing and handover costs in the network layer. Also, Xu *et al.* [5] address the handover problem in ultra-dense heterogeneous networks, focusing on a single-layer optimization where they can decrease the delay in the network. Since the problem is addressed from a single-layer perspective, the authors obtain slightly lower data rates than their reference model.

In this article, several multi-objective optimization problems have been formulated, tackling separately all pairwise combination of the capacity, signaling and power consumption objectives, plus a three-objective approach that considers them all simultaneously. The problems have been addressed by using Pareto-based multi-objective metaheuristics that compute a set of trade-off solutions to the problem, thus providing the decision maker (the network designer) with compromise network configurations.

The structure of this article is as follows. Section II presents the configuration of the system, detailing the different models used to compute the parameters and association strategies for assigning users to the base stations. In Section III, the optimization and network configuration are shown. Section IV analyzes the results obtained in the optimization. Finally, Section V provides the reader with the main conclusions drawn in this work and the future lines that remain open for future research.

II. SYSTEM MODEL

This section first describes the modeling of the target scenario, including both the base stations and the users of the network. Then, it details the formulation of the problem objectives, such as, capacity, power consumption, and signaling overhead. An availability indicator is also used to measure the demand satisfaction of the users in a given amount of time. Finally, the UE-BS association policy is included. The inputs and outputs of all models are combined to generate a comprehensive model based on the physical and network layers. This comprehensive model allows the realization of a multilayer optimization in Sections III and IV.

A. CONFIGURATION

The scenario comprises a working area of dimensions 500×500 m^2, where the BSs are distributed according to a uniform random distribution that is independent on each of the axes. These BSs are characterized into three possible cell types according to their size and operating frequency (macro, micro or femto). Their specifications are shown in Table 1. UEs are also randomly distributed around the terrain, but they move using a Random Waypoint Model (RWP), where their location, velocity and acceleration change over time. A graphical example of cell types and UEs movements in a scenario is illustrated in Fig. 1. According to the MIMO framework used, UEs may be equipped with two, three and four antennas, modelling low, medium and high demanding users, respectively.

As a traffic model between the UE and the BS, we assume that the session arrival follows a Poisson process with mean rate $\lambda = 0.2$. We also assume that the duration of a typical session is exponentially distributed with mean $\mu = 10$ s. In this scenario, BSs are connected to an access network where the routers offer IPv6 connectivity between mobile users and the rest of the deployed network.

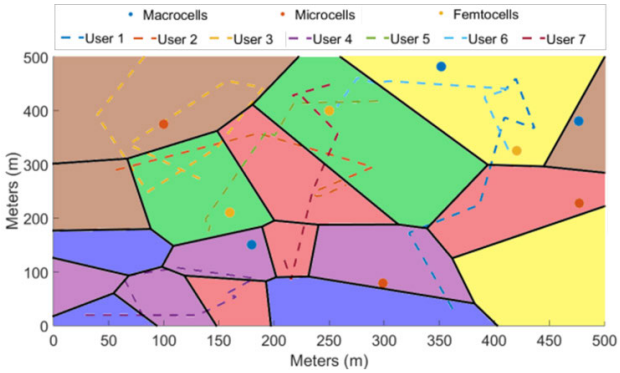

FIGURE 1. UEs and BSs in different propagation scenarios. Purple "UMA LOS", Blue "UMA NLOS" Green "UMi LOS", Red "UMi NLOS" Brown "RMa LOS" and Yellow "RMa NLOS".

TABLE 1. Specifications of the Base Stations.

	Macrocell	Microcell	Femtocell
Frequency (GHz)	2	5	28
Bandwidth (MHz)	10	25	140
Max Power (dBm)	46	25	20
Height (m)	25	10	6
BSs antennas	5	20	100

B. CAPACITY MODEL

First of all, the calculation of the power received (P_{RX}) by each user at each time t must be performed.

$$P_{RX}\,[\text{dBm}] = P_{TX}\,[dBm] + G\,[dB] + L_{PATHLOSS}[dB] \quad (1)$$

where P_{RX} and P_{TX} are the received and transmitted power, respectively, G is the sum of the gains of the transmitting and receiving antennas, and $L_{PATHLOSS}$ are the signal losses due to the transmission path that depend on the region where the signal is transmitted, as shown in Fig. 1. $L_{PATHLOSS}$ is computed as:

$$L_{PATHLOSS}\,[dB] = L_{SPACE}\,[dB] + L_{SHADOWFADING}\,[dB] \quad (2)$$

where L_{SPACE} are the signal losses due to the distance between UE and BS, decaying following an attenuation exponent n. $L_{SHADOWFADING}$ is the variation in $L_{PATHLOSS}$ due to multiple variables such as multipath propagation, the distribution of which follows a log-normal distribution. This distribution is given by an expected value μ and standard deviation σ that depend on the transmission models depicted below. Mathematically, L_{SPACE} can be seen as

$$L_{SPACE}\,[dB] = 20log_{10}\left(\frac{4\pi d_0}{\lambda}\right) + n10log_{10}\left(\frac{d}{d_0}\right) \quad (3)$$

where the first term computes the signal losses in free space until reference distance d_0 for a specific wavelength λ, and the second term considers how the signal decays at a distance d depending on the region with an attenuation exponent n.

Three transmission models are used in the experiment, UMi (Urban Microcells), UMa (Urban Macrocells) and RMa (Rural Macrocells) [26]–[28]. Fig. 1 shows how the terrain is divided according to different transmission models randomly. Each transmission model has also two possible cases, LOS (Line-Of-Sight) and NLOS (Non-Line-Of-Sight). They are assigned randomly to each region, making NLOS to appear more frequently in urban models, whereas LOS does in rural scenarios. The combination of models and cases results in six scenarios characterized by the attenuation exponent n, the expected value μ and the standard deviation σ.

Finally, the signal to interference plus noise ratio (SINR) has been calculated as follows:

$$SINR_k = \frac{P_{rx,j,k}(mW)}{(\sum_{\substack{n=1\\n\neq j}}^{M} P_{rx,n,k}\,(mW)) + P_{N_0}(mW)} \quad (4)$$

where $P_{rx,j,k}$ is the power received by user k from BS_j and $\sum_{\substack{n=1\\n\neq j}}^{M} P_{rx,n,k}$ is the total power received by user k from all the base stations M that work at the same frequency excepting BS_j, i.e., the interference. Finally, P_{N_0} is the noise power given by:

$$P_{N_0}\,[dBm] = -174 + 10\log_{10}(BW_j(MHz)) \quad (5)$$

where BW_j is the bandwidth available by the BS_j in MHz.

Once the SINR is obtained, the capacity of the channel can be calculated. The main aim when using MIMO is to improve the spectral efficiency by increasing the number of transmitters and receivers, resulting in better transmission conditions compared to a SISO system. This MIMO model is commonly used for studies of different nature, such as channel estimation [29], radiation pattern studies [30], or MIMO channel efficiency evaluations [31]. The capacity is computed for each time instant t due to the UEs movement. Eq. (6) is used for MIMO systems [29]–[32].

$$C_{k,j,t}\left(\frac{bits}{s}\right) = \frac{BW_{j,t}}{N_{j,t}}\log_2\left|I_j + \frac{SINR_{k,t}}{No.Rx_k} * H * H^H\right| \quad (6)$$

where $BW_{j,t}/N_{j,t}$ is the total bandwidth available to the user, and the $\log_2$ calculates the spectral efficiency in bits/s/Hz, where I_j is an identity matrix whose dimension is the number of transmitter antennas by BS_j and H is the channel matrix, which is generated randomly by using a complex normal distribution. The channel matrix dimensions are given by the number of antennas from users (rows) and base stations (columns).

C. POWER CONSUMPTION MODEL

One of the objectives of the optimization problem is the reduction of energy cost. Therefore, energy efficiency (EE) is an important parameter to define [33]. This indicator becomes fundamental in the deployment of new mobile generations due to the requirements of 90% reduction of power consumption. Nowadays, energy efficiency is a parameter to be taken into account in any new deployment [34], [35]. We have considered an EE indicator that shows the performance in bits per Joule, that is, the number of bits of information that can

be reliably transmitted through the communication channel per energy unit. It can be defined as:

$$EE\left(\frac{bits}{Joule}\right) = \frac{DataRate(bits/s)}{PowerConsumption(W)} \tag{7}$$

One of the main motivations for including EE issue is the fact that the theoretical limits of both the transmission data rates and the minimum latency are known: the Shannon limit and the speed of light, respectively. However, there is no known limit of the maximum energy efficiency that can be obtained in a network. In addition, Section IV will show how energy efficiency is a major distinguishing criterion to characterize the results.

Regarding the power consumption model, it takes into account both the consumption between UE and BS and the consumption between BS and the router in the access network. The power consumption of a BS, denoted as P_{bc}, can be expressed in the Aggregated Power Consumption Model [36] as:

$$P_{bc} = \alpha P + \beta + \delta S + \rho \tag{8}$$

where P represents the transmitted or radiated power of each BS and S is the data rate. The coefficient α denotes the power transmission efficiency due to an RF amplifier and supply losses, β represents the power dissipated due to signal processing, and δ is a constant denoting dynamic power consumption per data unit. These terms differ for different BS types defining a differential consumption model [37].

Detailing this model further, it can be seen that the power consumption can be therefore divided into three types. On the one hand, αP, the power consumption proportional to the transmission that depends directly on the power transmitted by the BS. On the other hand, δS, the power consumption proportional to the capacity that depends exclusively on the demand required by the user since it is directly linked to the data traffic. Finally, β and ρ represent fixed consumption terms.

Taking all this into consideration, the total power consumption in the system can be calculated as follows:

$$P_{Total} = \sum_{i=1}^{BS} M_i P_{bc} + P_{Backhaul} \tag{9}$$

where the first term is the sum of the powers of all base stations multiplied by the number of transmitting antennas corresponding to each base station, and $P_{Backhaul}$ represents the energy consumed by the backhaul. This latter has to be included to sum up the power consumption required to carry the signaling information from one region to another through the access network.

D. SIGNALING MODEL

To achieve an efficient service provisioning and a better usage of the network resources, 5G networks require to address issues not only in the radio and data link environment, but also in the layer 3 management protocols. Mobility management mechanisms allow reachability and maintain ongoing communication during roaming of mobile users in different networks. One of the key aspects in the performance of these protocols is related to the signaling, especially in densified networks, where high-speed mobile nodes experience frequent handovers with a high signaling load due to the short cell radius [38], [39].

Thus, for optimal system design, it is necessary to accurately model the impact of the mobility in other network parameters. In this work, we measure the impact of the mobility management on radio and link metrics. In current centralized solutions, the mobility management relies on an IP mobility anchor node, which is the network agent that tracks the network connection point of a user as the user moves. Whenever the user changes their point of attachment to the network, the user registers with this agent through signaling messages informing of its current location. As a result of this signaling exchange, the Mobile Node (MN) acquires a new IP address in this foreign network.

In mobility management protocols [40], [41], this anchor node is the centralized part of the system since it is on the critical path of both signaling and data for mobile users. Regarding the signaling, a mobility management protocol requires that an MN sends a location update to its mobility anchor whenever it moves from one subnet to another. This location registration is required even though the MN does not communicate with others while moving. The signaling cost associated with location updates may become very significant as the number of MNs increases.

Moreover, this cost depends on the size in bytes of the signaling messages (s_u) and the number of hops between the MN and the mobility anchor ($h_{MN-anchor}$) in every handover process during the time interval that the MN communication remains active. Thus, we refer to the aggregate signaling cost of registration update for a session as C_s and it is expressed as:

$$C_s = s_u h_{MN-anchor} N_h \tag{10}$$

where N_h is the number of handovers that cause a layer 3 handover.

E. AVAILABILITY MODEL

Availability is defined as the probability of a user demand to be fulfilled at a given time. This parameter turns out to be of vital importance because in many occasions the total capacity provided is not sufficient to meet the user requirements. This fact will depend on whether his demand is satisfied by the capacity, so availability in the model is computed as

$$Availability_k = P\{C_k \geq D_k\} \tag{11}$$

where C_k is the capacity for the user k and D_k are the demands from the user k. Total availability in the system is computed as an average of every user present in the scenario.

$$Availability_{Total} = \frac{\sum_{i=1}^{k} Availability_k}{N} \tag{12}$$

F. BS-UE ASSIGNMENT

Two policies for pairing UEs and BSs have been devised, being they two aimed at maximizing SINR. Other criteria could have been used, such as minimizing the distance or maximizing the power received between UE and BS. However, the maximization of the SINR is the one usually applied in actual network deployments. The two strategies are:

- Planning 1: the UE is paired with the BS that provides the highest SINR out of all those available in the scenario, regardless its type.
- Planning 2: the aim is to avoid continuous handovers between BSs. As so, it pairs the UE with the BS that provides the highest SINR among all those available in the scenario, but only when the change leads to an improvement in the SINR above a certain threshold.

III. MULTILAYER NETWORK OPTIMIZATION

A. NETWORK CONFIGURATIONS

Two different configurations have been devised. A light setting with 20 UEs and 5 BSs, and a heavy one with 50 UEs and 20 BSs, respectively. From now on, the first configuration will be mentioned as light configuration, and the second one as heavy configuration. These configurations distribute the propagation models randomly as shown in Fig. 1. Moreover, the type of UEs and BSs are also uniformly distributed.

B. OPTIMIZATION PROBLEM

This section clearly states the optimization problem addressed in this work. First, the decision variables that define the problem are the transmitted powers of the BSs, which fully impacts all the optimization objectives defined in the previous section. Indeed, it clearly determines the power consumption of the network (eq. (9)). As it also directly changes the SINR, because it modifies the power received by the users (eq. (4)) and, hence, the data rates provided by the network (eq. (6)) and the cell limits, inducing a different number of handovers, thus modifying the signaling cost. Moreover, the availability changes if the data rates changes. As it can be seen, updating the transmission power of just one single base station may provoke changes in the values of all the objectives.

Given the problem difficulty, with a severe epistasis among the decision variables, and the potential large scale of the instances of the ultradense deployments, we have relied on metaheuristics [42] as optimization tools. More concretely, evolutionary multi-objective algorithms (MOEAs) have been used [43] because, on the one hand, they can approximate the Pareto front of a problem in one single run and, on the other hand, as randomized black-box optimizers, they can address optimization problems with nonlinear, non-differentiable or noisy objective functions. The objectives to be optimized are those shown in Section II, namely, capacity, power consumption, signaling cost and availability.

In this way, the optimization problem is mathematically formulated as follows: Let B be the set of the deployed Base Stations (BTSs). A solution to the presented problem is then a real-valued vector, $s \in (0, 1]^{|B|}$, where s_i indicates the transmitted power of BTS i. Thus, the four objectives functions are:

$$\begin{aligned} f_1(s) &= \min\ PowerConsumption(s) \\ f_2(s) &= \max\ Capacity(s) \\ f_3(s) &= \min\ SignalingCost(s) \\ f_4(s) &= \max\ Availability(s) \end{aligned}$$

which are grouped and combined resulting in several multi-objective optimization problems.

C. ALGORITHMS

A brief technical description of the each of the algorithms used to address the problem is provided in the following. Note that in order to measure the quality of the approximated fronts given by the algorithms, the hypervolume indicator (HV) was used, which is recognized as one of the most suitable Pareto-compliant metrics in the multi-objective community [44]. Higher values of this indicator are better.

- NSGAII: The Non-Dominated Sorting Genetic Algorithm II [45] is a genetic algorithm based on generating a new population from the original one by applying the typical genetic operators (selection, crossover, and mutation); then, the individuals in the new and old population are sorted according to their rank, and the best solutions are chosen to create a new population.
- SMPSO: SMPSO [46] is a multi-objective particle swarm optimization algorithm in which global best particles are generally the non-dominated solutions found during the particle movement and they can be exploited to guide the particle swarm to approach the entire Pareto Front.

All the two algorithms use Polynomial Mutation as mutation operator, with a probability of 0.01. In the case of NSGAII, SBXCrossover with crossover rate of 0.9 is also used.

IV. RESULTS

In order to provide the results with confidence, 30 independent runs of the MOEAs have been carried out. Also, thorough statistical procedures have been used [47] with a confidence level of 95% (p-value < 0.05). The p-value obtained for the multcompare test is 1.5229e-06. The results of this procedure have shown that all the differences are statistically significant, thus pointing out that the HV of SMPSO is statistically greater (better) than that of NSGA-II and the MatLab algorithms. The results have been analyzed in terms of the empirical attainment functions (EAF) [48] and the best aggregated front among all the non-dominated solutions found in all the 30 runs. The EAD used here is the 50%-attainment surface in the multi-objective domain that is analogous to the median value in the single-objective one.

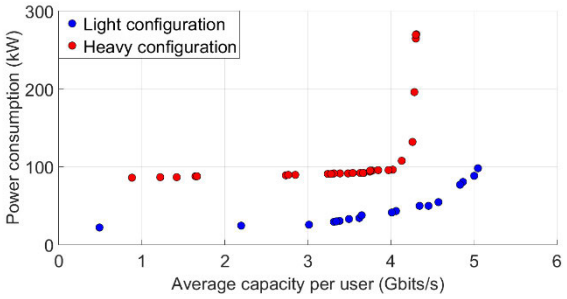

FIGURE 2. Pareto front of the average capacity per user against power consumption. Results obtained for planning 1 in both heavy and light configurations.

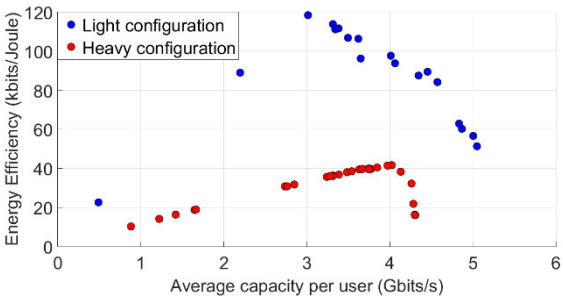

FIGURE 3. Energy efficiency of the Pareto front of the average capacity per user against power consumption. Results obtained for planning 1 in both heavy and light configurations.

A. JOINT OPTIMIZATION OF CAPACITY AND POWER CONSUMPTION

The first experiment carried out considers two objectives: the capacity per user and the power consumption. The results show the average over time of the capacity for every UE. Similarly, they show the power consumption for every BS. Both light and heavy configurations have been considered. The assignment UE-BS selected is planning 1.

Fig. 2 shows the average capacity that a user can reach for the lowest power consumption that can provide that capacity. It can be concluded that heavier configurations need to use larger amounts of power to fulfill the user data rates demanded by each user. This behavior can be explained from two points of view. On the one hand, the number of UEs is larger in the heavy configuration. Therefore, the number of BSs has to be larger to obtain the same capacity per user, and the transmitted power will be larger for a larger number of BS. On the other hand, the more UEs and BSs, the more interference is generated in the system for the same scenario, which implies difficulties to provide the same service.

The benefits of having such an approximated Pareto front is that the decision maker can easily choose whether s/he desires to lose the capacity to save power, or conversely to provide the maximum possible capacity at the expense of power savings. One of the ways to find the balance between these two parameters can be obtained representing the relationship among themselves, the energy efficiency, as it can be observed in Fig. 3. This illustrates EE in the capacity range. The horizontal axis is the same as in Fig. 2, so that the vertical axis is scaled by normalizing it with respect to the horizontal axis and thus obtaining the EE. Therefore, the maximum point in terms of EE for both light and heavy strategies could be considered as an optimal operation point.

Fig. 3 shows how the most efficient points are those with an average capacity of around 3 Gbps for the light configuration and 4 Gbps for the heavy configuration. In addition, it can be clearly seen how the light configurations work better than the heavy configurations. Finally, it shows the differences in efficiency are greater in the light configurations.

From this point on, only light configuration has been used (in this section and in the others as well). The solutions with higher energy consumption have also been limited. As it can be seen in Fig. 3 the energy efficiency falls drastically at these points and we are not interested in working on these points.

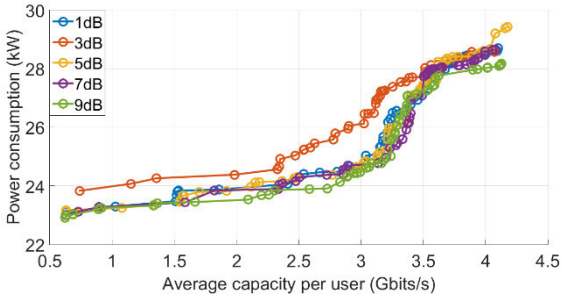

FIGURE 4. Pareto front of the average capacity per user against power consumption for several fixed thresholds. Results obtained for planning 2 in the light configuration. Best aggregated value.

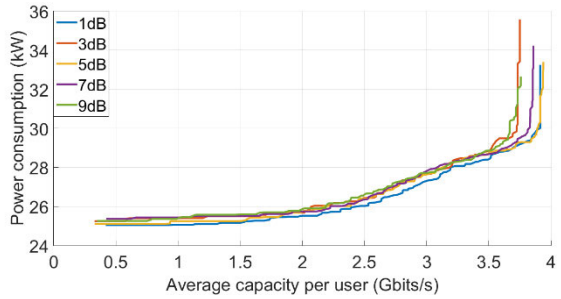

FIGURE 5. Pareto front of the average capacity per user against power consumption for several fixed thresholds. Results obtained for planning 2 in the light configuration. Average.

Now, the planning strategy (BS-UE assignment) is changed to evaluate its impact. The optimization is done separately with 5 different threshold values (1, 3, 5, 7 and 9 dB). The approximated Pareto fronts for the fixed threshold values are shown in Figs. 4 and 5. The results represent the best aggregated non-dominated solutions of the 30 runs of each threshold case in Fig. 4, whereas the attainment functions are depicted in Fig 5. Looking at Fig. 4, the results show similar results for the different thresholds, except for 3 dB (orange line), which is slightly worse. Despite the range between 3.2 and 3.5 Gbits/s, the best approximated front is when the threshold is equal to 9 dB. However, when moving to the average fronts in Fig. 5, the differences among thresholds

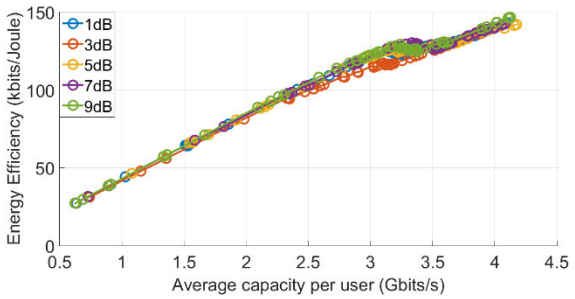

FIGURE 6. Energy efficiency of the Pareto front of the average capacity per user against power consumption for several fixed thresholds. Results obtained for planning 2 in the light configuration.

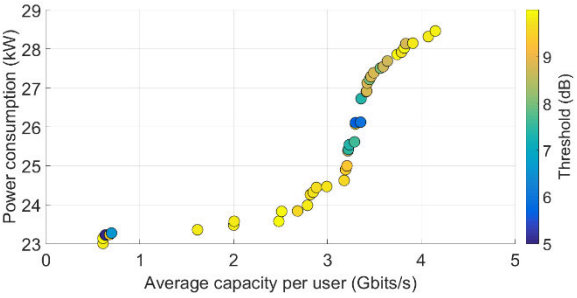

FIGURE 7. Pareto front of the average capacity per user against power consumption when the threshold is optimized. Results obtained for planning 2 in the light configuration.

diminish. In this figure, the blue line that represents a threshold of 1 dB is slightly better. This indicates that the algorithm can more easily find solutions with that threshold since average optimal results are achieved by the lowest threshold. In contrast with Fig. 4 where the best Pareto front results are found with a threshold of 9 dB. This fact indicates the need for a high computing workload to approach the average results towards the best aggregated values.

As it is explained in Section II.C, the merit factor accepted by the scientific community, EE (bits/Joule), eases the comparison of different solutions of a given approximation to Pareto front. In order to obtain the maximum limit of the energy efficiency, the values have been obtained from the aggregated Pareto fronts (see Fig. 4). Thus, Fig. 6 illustrates the energy efficiency for several thresholds, which are very similar among them. The only remarkable difference appears, again, in the central part of the graph, between 3 to 3.5 Gbits/s, where it seems that the slope decreases and the orange line (3 dB) is clearly below.

To obtain more information about the effects of the threshold on the network parameters, a new experiment has been conducted, but now including a threshold parameter as a decision variable to be optimized. The results obtained in this case are illustrated in Figs. 7 and Fig 8.

Fig. 7 depicts the approximated Pareto front when the threshold is taken into consideration. It also displays a color scale on the right part of the plot to show the threshold value computed by the algorithm for each of the non-dominated solutions reached. It can be observed that all these solutions

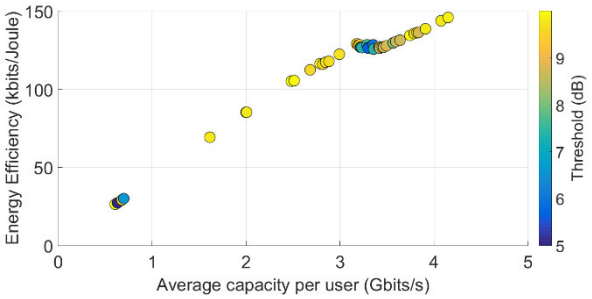

FIGURE 8. Energy efficiency of the Pareto front of the average capacity per user against power consumption when the threshold is optimized. Results obtained for planning 2 in the light configuration.

have always obtained thresholds above 5 dB. A second interesting finding arises when the capacity is roughly 3.2 Gbits/s, where a sharp increase in the power consumption occurs. This is a very valuable information for the network designer (decision maker) as s/he can significantly reduce the energy consumption of the network, penalizing minimally its capacity. As it can be seen, at this point the algorithm tries different values for the threshold around 7 dB, without finding a better performance in terms of capacity without increasing power consumption. At a first glance, if only Fig. 7 is considered, it may seem reasonable to work at operating points below 3 Gbps. However, observing the energy efficiency in Fig. 8, the true fact is that the solutions near 4 Gbits/s do have the higher energy efficiency. This is due to the fact that the increase in energy consumption is counteracted by the rapid increase in capacity, so that in terms of efficiency, the increase in capacity is bearable at the expense of the additional transmission power required. It is also important to note from Fig. 8 that in the zone where the algorithm does not find suitable solutions (3 to 3.5 Gbits/s approximately) the trend of energy efficiency changes showing that best efficiencies are in accordance with Fig. 7.

B. JOINT OPTIMIZATION OF SIGNALING COST AND CAPACITY

The second experimentation is the joint optimization of data rates and signaling cost. As explained above, signaling cost is the accumulative layer 3 mobility signaling overhead for supporting mobility service for a user. This metric is directly proportional to the number of hops between the mobility anchor and the user and also to the total number of handovers. Therefore, the reduction of this cost implies an overall reduction in the handover latency. Therefore, the aim of this second experiment is to target a possible 6G scenario where ultra-low latency and very high transmission data rates are required.

In a similar way to the previous section, the variables to be optimized are the transmitted power at the base station and the optimization is performed for fixed thresholds. Fig. 9 shows the aggregated front of the non-dominated solutions reached in the 30 independent runs. It can be seen that higher thresholds obtain the approximated fronts that converge the most. It has to be clarified that, a zero signaling cost indicates that

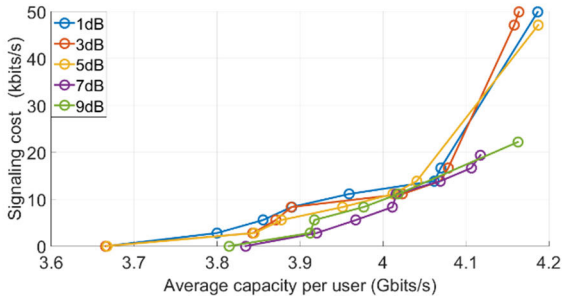

FIGURE 9. Pareto front of the average capacity per user against signaling cost for several fixed thresholds. Results obtained for planning 2 in the light configuration. Best aggregated value.

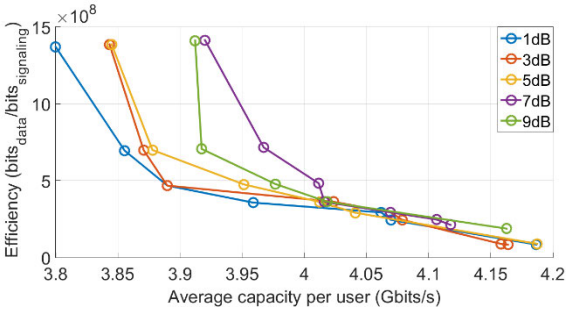

FIGURE 10. Efficiency ($bits_{data}/bits_{signaling}$) of the Pareto front of the average capacity per user against signaling cost for several fixed thresholds. Results obtained for planning 2 in the light configuration.

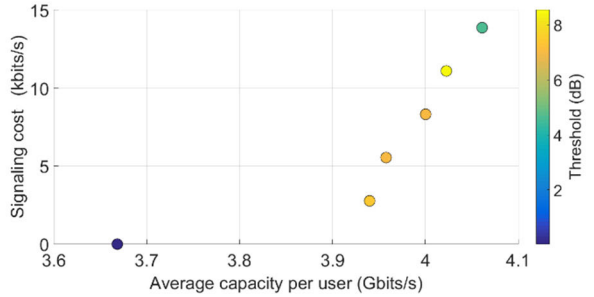

FIGURE 11. Pareto front of the average capacity per user against signaling cost when the threshold is optimized. Results obtained for planning 2 in the light configuration.

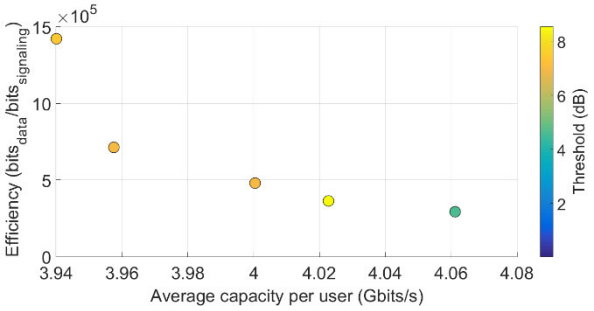

FIGURE 12. Efficiency ($bits_{data}/bits_{signaling}$) of the Pareto front of the average capacity per user against signaling cost when the threshold is optimized. Results obtained for planning 2 in the light configuration.

the user remains in the same cell throughout the simulation, sacrificing capacity at the cost of decreasing latency. In order to further analyse the information enclosed in the approximated fronts, similar to the merit factor shown previously (EE), this work proposes for the first time, and to the best of our knowledge, a merit factor that provides the ratio of data sent for each signaling bit used (if no signaling is generated because no handover occurs, the metric remains undefined).

Fig. 10 shows the results, which indicates that lower capacities obtain higher efficiencies in terms of signaling bits sent through the network per data bit. It can be therefore concluded that it is more interesting to work at operation points with low signaling. From the results, it can be seen that a high threshold is required to obtain the highest values in our merit factor (green and purple lines) since they obtain same merit factor for larger capacities.

In a similar way to the previous section, an optimization with a threshold as the variable is done. Figs. 11 and 12 show capacity-signaling cost optimization when the threshold value is a decision variable for the best aggregated value in order to see the maximum performance of the network. Similar to Fig. 9, Fig. 11 reveals that the higher capacity incurs the higher signaling cost. This is explained by the fact that to obtain maximum capacity, the user has to be constantly moving between those BSs that provide the best SINR, which incurs in signaling cost, and therefore, higher latencies. Moreover, paths followed by the signaling traffic are fixed. For that reason, it is not possible to find a large number of solutions in the Pareto front.

To conclude this section, it can be said that high thresholds produce better results than low thresholds. It should also be noted that the cost of signaling vary much more strongly than the capacities in relative terms. Finally, it is more convenient to work in the area of low signaling as it is shown in Fig. 12.

C. JOINT OPTIMIZATION OF SIGNALING COST AND POWER CONSUMPTION

In this section, a power consumption-signaling cost optimization is carried out following the methodology of the previous ones. Figs. 13 and 14 show the best aggregate and average value of the 30 simulations respectively. In these figures, it can be seen how the high threshold values (green and

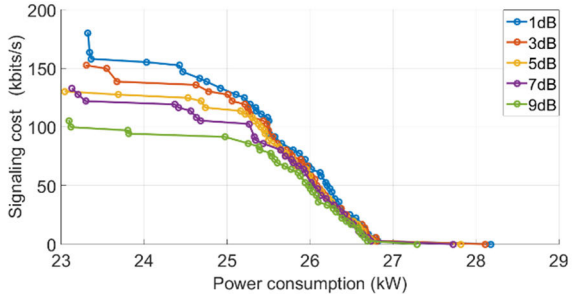

FIGURE 13. Pareto front of the power consumption against signaling cost for several fixed thresholds. Results obtained for planning 2 in the light configuration. Best aggregated value.

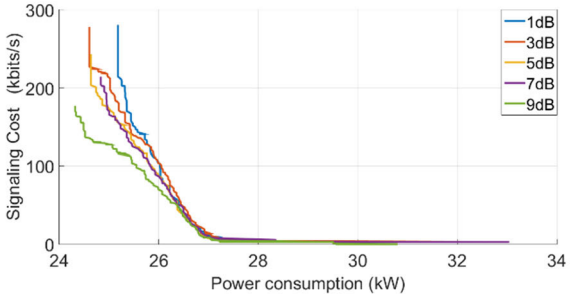

FIGURE 14. Pareto front of the power consumption against signaling cost for several fixed thresholds. Results obtained for planning 2 in the light configuration. Average.

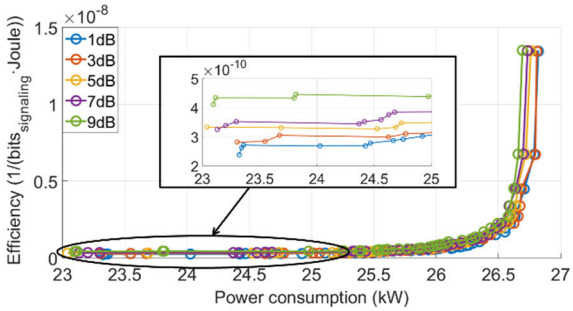

FIGURE 15. Efficiency ($1/(bits_{signaling} \cdot Joule)$) of the Pareto front of the power consumption against signaling cost for several fixed thresholds. Results obtained for planning 2 in the light configuration.

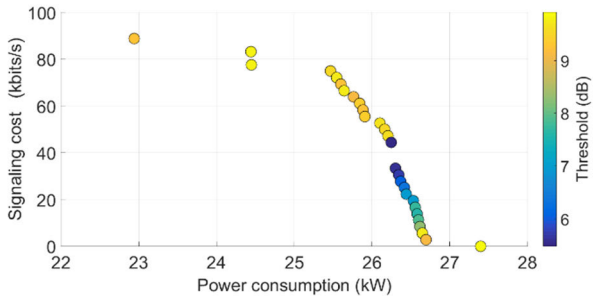

FIGURE 16. Pareto front of the power consumption against signaling cost when the threshold is optimized. Results obtained for planning 2 in the light configuration.

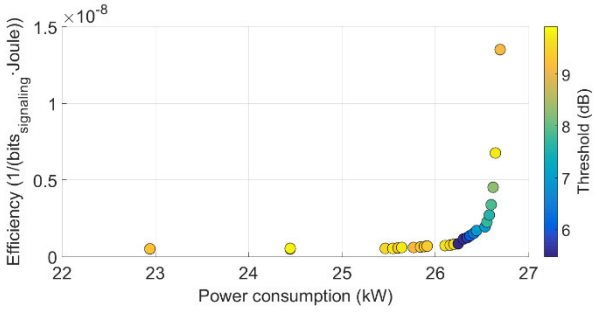

FIGURE 17. Efficiency ($1/(bits_{signaling} \cdot Joule)$) of the Pareto front of the power consumption against signaling cost when the threshold is optimized. Results obtained for planning 2 in the light configuration.

purple) work much better. Furthermore, the differences are much more pronounced for lower power consumption values. The higher power consumption incurs in lower signaling cost. The increase in the transmitted power by BSs decreases the number of handovers since the users tend to stay connected to the same BS.

In a similar way to the previous sections, a new merit factor that can compare the different points on the Pareto front is proposed. This new merit factor is the inverse of the watts consumed multiplied by the signaling cost. This merit factor will indicate the joint cost of the signaling and the power consumption and it will show the best operation points. Thus, Fig. 15 shows this new merit factor. In line with the previous figures, the best values of the new merit factor are obtained for the higher thresholds. This trend is shown across the entire range of power consumption. It can be seen how the most efficient working points are for the highest power consumed.

To follow the same structure as in the previous sections, optimization is carried out with the threshold as another decision variable in the optimization. The results are shown in Figs. 16 and 17. Fig. 16 presents the best Pareto front and Fig. 17 presents the merit factor. The results show how in the extremes of power consumption, the algorithm always chooses very high values for the threshold. This is in line with Figs. 13 and 14 where it can be seen that the differences between the different thresholds are greater at the extremes.

D. TRI-OBJECTIVE OPTIMIZATION PROBLEM

From the previous sections, it can be seen how when comparing data rates and power consumption, the best operation points are for high data rates. However, when comparing signaling cost and data rates, the optimum operation points are at low data rate points. Therefore, these operation points are contradictory and a joint optimization of the three factors is necessary in order to draw conclusions. Therefore, a combination of the three previous optimizations is made, where a surface is obtained as Pareto front as it is a three-dimensional optimization. Fig. 18 depicts this optimization and three trends can be distinguished. Signaling is minimized for low capacities and high power consumptions. Capacity is maximized for high power consumptions and high signaling. Power consumption is minimized for low capacities and high signaling.

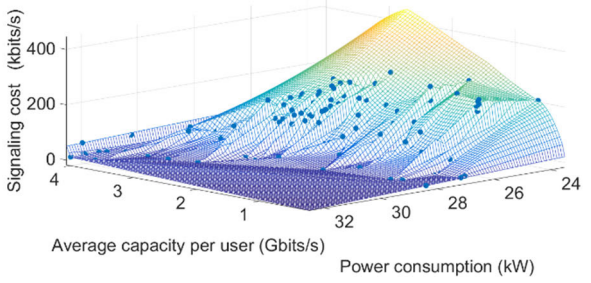

FIGURE 18. Pareto front of average capacity per user against power consumption against signaling cost. Results obtained for planning 1 in the light configuration.

Finally, a merit factor that takes into account the three network parameters simultaneously (data rates, power

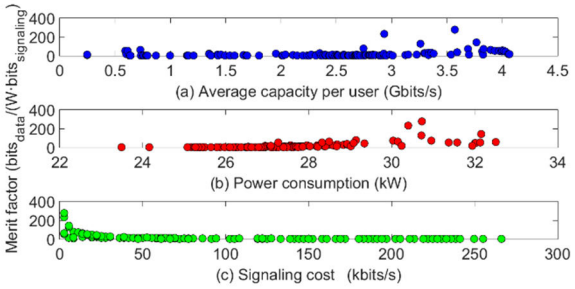

FIGURE 19. Merit factor ($bits_{data}/(W \cdot bits_{signaling})$) as a function of: (a) data rate, (b) power consumption and, (c) signaling cost.

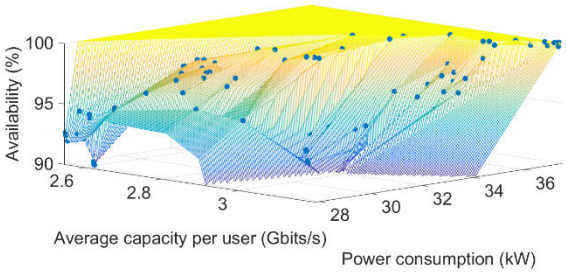

FIGURE 20. Pareto front of average capacity per user against power consumption against availability. Results obtained for planning 1 in the light configuration.

consumption and signaling cost) is proposed. This merit factor is calculated by dividing the data bits by the power consumed and the signaling bits. It reveals how many data bits can be sent with a watt of power and one bit of signaling. Fig. 19 shows this new merit factor as a function of average capacity in Fig. 19(a), as a function of power in Fig. 19(b) and as a function of signaling in Fig. 19(c). In these figures, it can be seen that the highest efficiencies of this merit factor are given for medium-high capacity and power values (around 3.5 Gbits/s and 30 to 31 kW). Also, in accordance with the previous sections, the best operations points are those found for low signalization values.

In addition, Fig. 20 shows a three-dimensional optimization that involves capacity, power consumption and availability. Taking into account availability is another key factor since the user should have coverage in order to satisfy his requirements. Total availability is obtained for high power consumptions where higher SINRs are able to improve the capacity, and therefore the data rate.

E. NSGAII AND SMPSO TRI-OBJECTIVE OPTIMIZATION PROBLEM

The previous section shows the study of the objectives with the default algorithm used by MatLab. Going further as explained in Section III, this study is performed with two additional algorithms, NSGAII and SMPSO. These allow us to go deeper into the tri-objective optimization case and extend results depending on the algorithm used. Ten iterations have been performed for each algorithm. The figures shown throughout this section show a representative description of the set of all the iterations.

Following the idea proposed in Fig. 18, a representation of the three-dimensional Pareto front is drawn in Fig. 21 for each of the three algorithms applied. On the one hand, the front of NSGAII differs slightly from the original MatLab front. On the other hand, the front proposed by SMPSO is quite different from the two previous ones.

In order to study these results further, the objectives are divided into three two-dimensional planes presented in Fig. 22. The first column, which draws the signaling as a colour scale, shows that NSGAII and SMPSO achieve better results than MatLab. NSGAII finds a space of solutions with lower energy consumption (objectives are shifted downwards) and less signaling (colder colors). In SMPSO it is remarkable that a set of low signaling cost objectives is found. They minimize energy consumption and signaling cost in exchange for lower average capacity per user. This set of objectives at the bottom left would be the example of a conservative deployment. The second column represents the power consumption as a colour scale. NSGAII gets colder colours since it is the algorithm with the best solutions in terms of energy saving. SMPSO concentrates the objectives in high

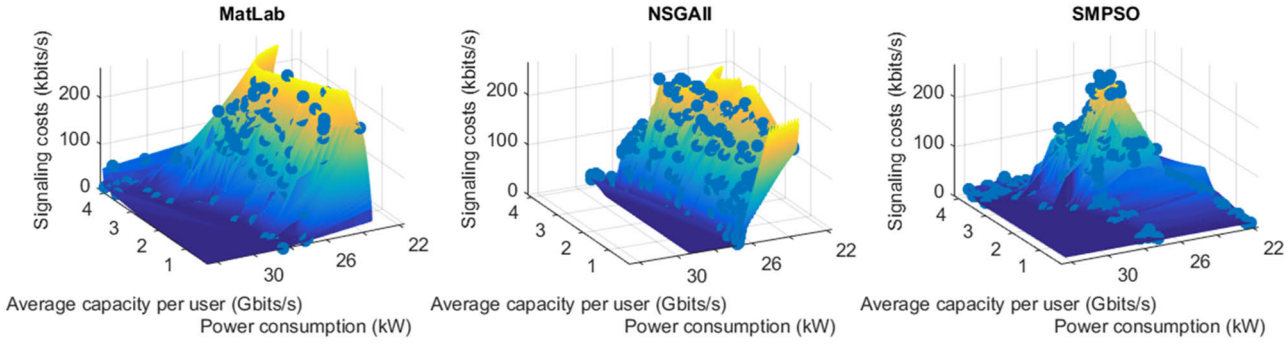

FIGURE 21. Pareto fronts of average capacity per user against power consumption against signaling costs. Optimization algorithms are default in MatLab, NSGAII and SMPSO. Results obtained for planning 1 in the light configuration.

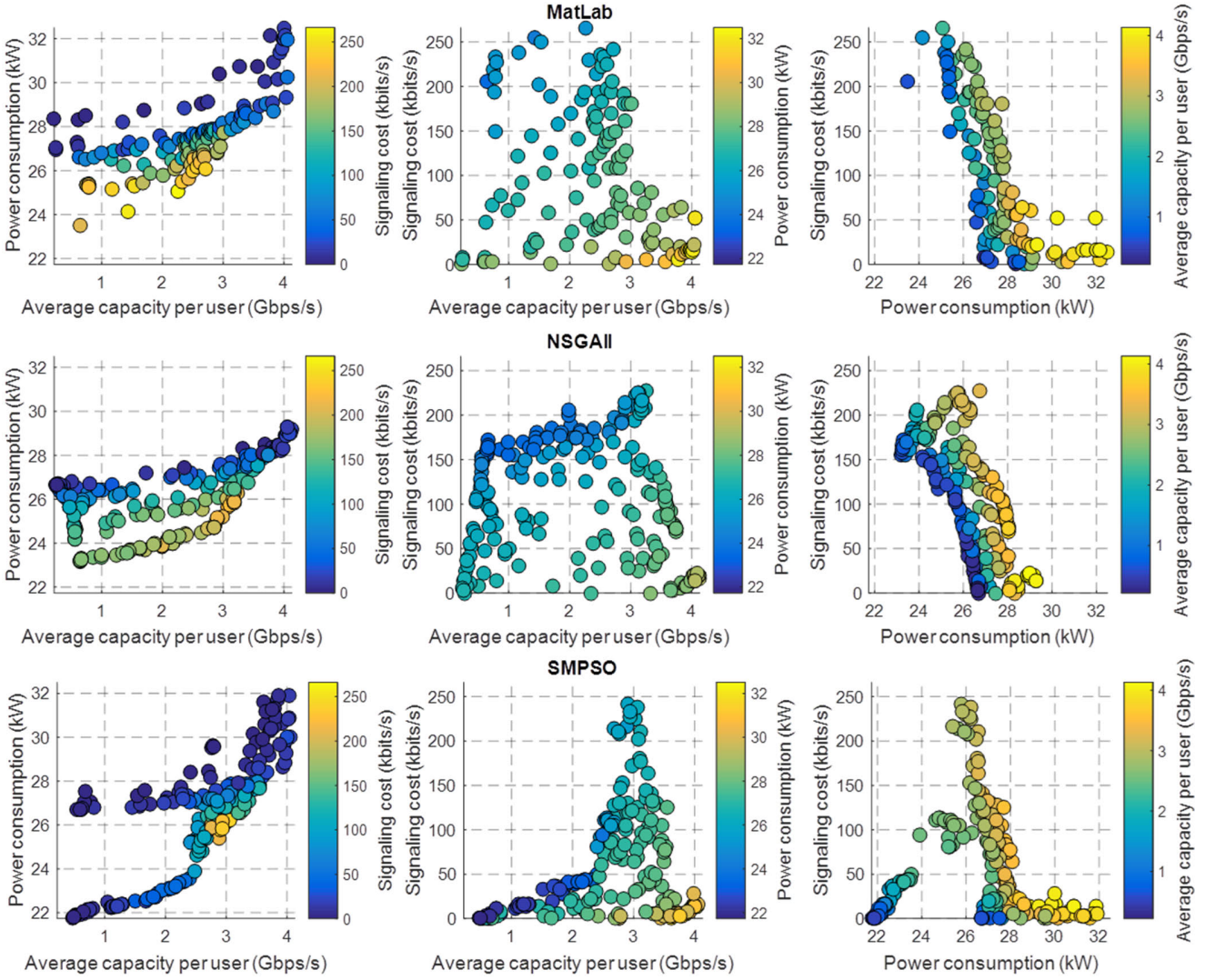

FIGURE 22. Two-dimensional representation of the Pareto fronts. First, second and third rows represent MatLab, NSGAII and SMPSO algorithms respectively. First, second and third column represent signaling costs, power consumption and average capacity per user as a colour scale.

TABLE 2. Hypervolume Comparison.

	MatLab	NSGAII	SMPSO
Hypervolume	0.39259	0.48809	0.61668

capacity areas except for a small section corresponding to the conservative case explained above.

Finally, the third column draws the power average capacity per user as a colour scale. By the same reasoning as above, NSGAII objectives are shifted to the left, corresponding to more energy efficient areas for similar capacities and signaling. SMPSO explores a new area at the bottom left corresponding to the conservative case.

The previous analysis of the Fig. 22 can be completed with another analysis using performance metrics such as hypervolume. Table 2 shows the average hypervolume for all iterations of each algorithm.

In terms of hypervolume, the best algorithm is SMPSO, followed by NSGAII in second place, and finally MatLab. The explanation is similar to that given in Fig. 22. On the one hand, NSGAII improves on MatLab with decreases in power consumption. On the other hand, SMPSO explores Pareto front areas that are not analyzed in the two previous algorithms. This case allows a more complete view of the Pareto front, which maximizes the hypervolume.

F. BASELINE COMPARISON

The hypervolume indicator shows the best Pareto fronts in a very compact way. However, it does not allow to see the improvement from the starting point. A visual comparison with the baseline can be made. The baseline used for the study consists on the average capacity per user, signaling cost and power consumption objectives when all BSs are operating at maximum power. This operation point provides the following results: 2.51 Gbps (average capacity per user),

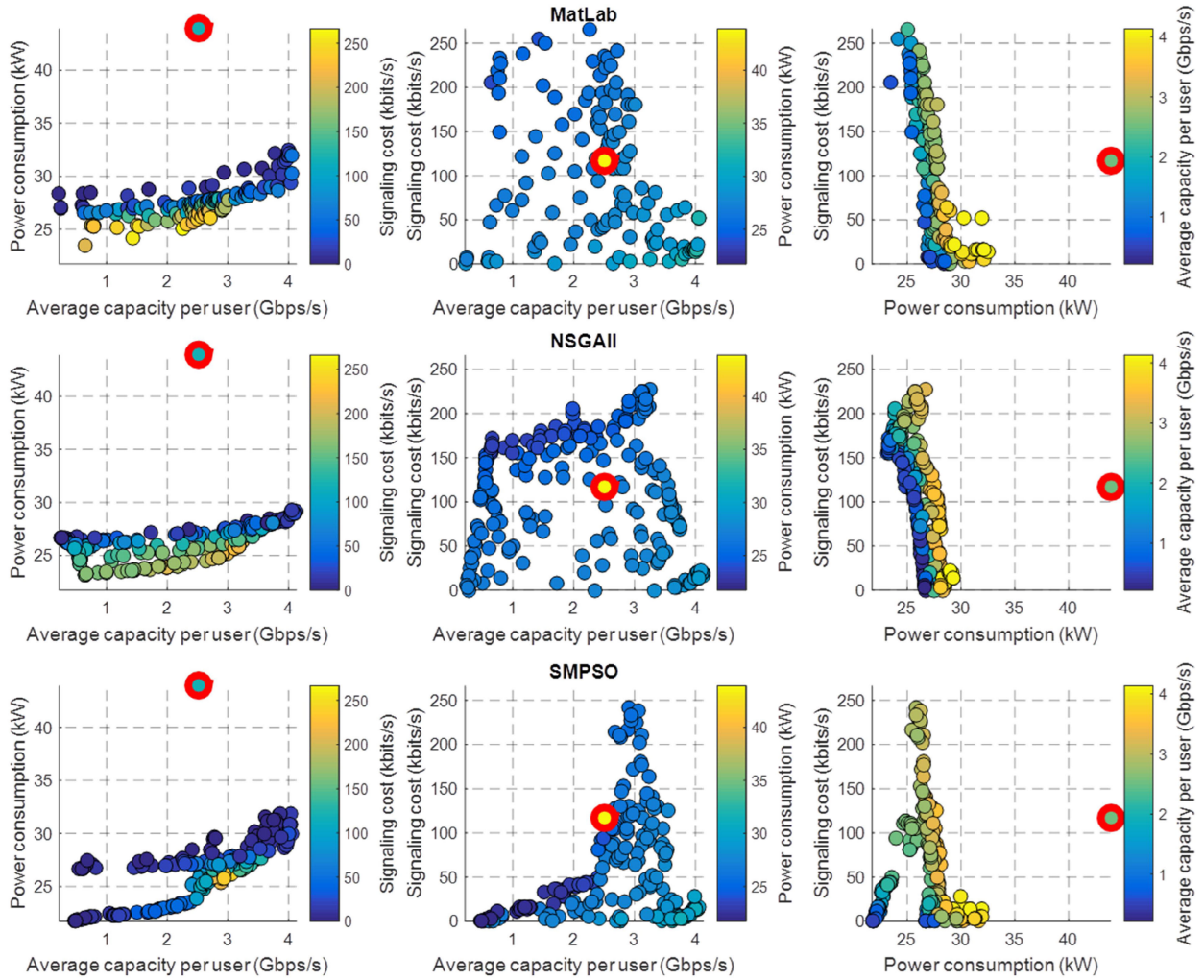

FIGURE 23. Baseline in the two-dimensional representation of the Pareto fronts. First, second and third rows represent MatLab, NSGAII and SMPSO algorithms respectively. First, second and third column represent signaling costs, power consumption and average capacity per user as a colour scale.

43.9 kW (power consumption) and 116.5 kbps (signaling cost). Fig. 23 shows the operating point of the baseline on the Pareto fronts obtained for the three algorithms. In the first column it is clear that the power consumed in the deployment is improved, going from 43.9 kW to values in the range of 23 kW to 33 kW. The second column shows that the baseline obtains intermediate values in terms of signaling and capacity. However, the yellow color of the baseline indicates that the power consumed to obtain these capacities and signaling is much higher than the rest of the objectives on the fronts. Finally, the third column shows a performance similar to the first one, where the power consumed is much higher than the Pareto front.

V. CONCLUSION

In this work, we have presented a multilayer network optimization that optimizes some performance criteria. The comprehensive model, based on the physical and network layers, allows the multilayer optimization where all objectives are improved simultaneously. UEs capacity and BSs power consumption from the network layer are optimized. UEs signaling bits due to handovers in the network from the data link layer are also considered in the optimization. These optimizations are reflected in Pareto fronts, which show a set of non-dominated solutions to the problem. They keep a trade-off that provides the network designer with a set of optimal settings for the network deployment. In order to decide a certain configuration, the calculation of efficiency parameters, such as energy efficiency, has also been carried out, showing the optimum operating point for the network. To go deeper into finding the optimal working point, three new merit factors have been proposed that take into account different parameters of the network.

The analysis of the merits factors shows the optimal operation points. These points can be useful for the telecommunication companies in order to allow new services with high performance in all parameters. Therefore, the new merits factors play a fundamental role in finding the balance

between the different criteria assessed. Pareto fronts have been obtained from three different optimization algorithms. The comparison with the baseline shows that these Pareto fronts are able to improve multiple objectives simultaneously. The hypervolume analysis indicates that SMPSO presents the best objectives on the Pareto front.

As a future direction, D2D communications and multi-access edge computing (MEC) could improve the performance indicators since these technologies decrease the signaling costs and power consumption on the scenario due to the cooperation among close users. Moreover, the statistical multiplexing could increase the benefits of the optimization by coordinating several streams simultaneously. Although this technique slightly increases signaling traffic in the network, this is offset by the potential resource savings in terms of spectrum allocation.

5G and 6G aim to substantially improve all these QoS metrics simultaneously. To this end, this study has easily illustrated the trade-off between these performance indicators reached by three multi-objective optimization algorithms.

REFERENCES

[1] Ericsson. (2019). *Ericsson Mobility Report November 2019*. [Online]. Available: https://www.ericsson.com/4acd7e/assets/local/mobility-report/documents/2019/emr-november-2019.pdf

[2] Cisco. (2020). *Cisco Annual Internet Report (2018-2023)*. [Online]. Available: https://www.cisco.com/c/en/us/solutions/collateral/executive-perspectives/annual-internet-report/white-paper-c11-741490.html

[3] E. Steinbach, M. Strese, M. Eid, X. Liu, A. Bhardwaj, Q. Liu, M. Al-Ja'Afreh, T. Mahmoodi, R. Hassen, A. El Saddik, and O. Holland, "Haptic codecs for the tactile Internet," *Proc. IEEE*, vol. 107, no. 2, pp. 447–470, Feb. 2019.

[4] Z. Xiang, F. Gabriel, E. Urbano, G. T. Nguyen, M. Reisslein, and F. H. P. Fitzek, "Reducing latency in virtual machines: Enabling tactile Internet for human-machine co-working," *IEEE J. Sel. Areas Commun.*, vol. 37, no. 5, pp. 1098–1116, May 2019.

[5] X. Xu, X. Tang, Z. Sun, X. Tao, and P. Zhang, "Delay-oriented cross-tier handover optimization in ultra-dense heterogeneous networks," *IEEE Access*, vol. 7, pp. 21769–21776, 2019.

[6] A. Gorbenko, O. Tarasyuk, A.-L. Kor, and V. Kharchenko, "Green economics: A roadmap to sustainable ICT development," in *Proc. IEEE 9th Int. Conf. Dependable Syst., Services Technol. (DESSERT)*, Kiev, Ukraine, May 2018, pp. 561–567.

[7] M. M. Martino, G. Mutani, M. M. Pastorelli, and M. R. Miceli, "Smart energy users: ICT instruments for the consumer awareness," in *Proc. IEEE Int. Telecommun. Energy Conf. (INTELEC)*, Osaka, Japan, Oct. 2015, pp. 1–6.

[8] *Summary of Rel-15 Work Items*, document TR 21.915, 3GPP, 2018.

[9] V. Wong, R. Schober, D. W. K. Ng, and L. Wang, *Key Technologies for 5G Wireless Systems*. Cambridge, U.K.: Cambridge Univ. Press, 2017.

[10] X. Chen, D. Wing Kwan Ng, W. Yu, E. G. Larsson, N. Al-Dhahir, and R. Schober, "Massive access for 5G and beyond," 2020, *arXiv:2002.03491*. [Online]. Available: http://arxiv.org/abs/2002.03491

[11] T. Han and N. Ansari, "A traffic load balancing framework for software-defined radio access networks powered by hybrid energy sources," *IEEE/ACM Trans. Netw.*, vol. 24, no. 2, pp. 1038–1051, Apr. 2016.

[12] J. Heinonen, P. Korja, T. Partti, H. Flinck, and P. Poyhonen, "Mobility management enhancements for 5G low latency services," in *Proc. IEEE Int. Conf. Commun. Workshops (ICC)*, Kuala Lumpur, Malaysia, May 2016, pp. 68–73.

[13] D. Lopez-Perez, M. Ding, H. Claussen, and A. H. Jafari, "Towards 1 Gbps/UE in cellular systems: Understanding ultra-dense small cell deployments," *IEEE Commun. Surveys Tuts.*, vol. 17, no. 4, pp. 2078–2101, 4th Quart., 2015.

[14] Z. Pi and F. Khan, "An introduction to millimeter-wave mobile broadband systems," *IEEE Commun. Mag.*, vol. 49, no. 6, pp. 101–107, Jun. 2011.

[15] E. G. Larsson and L. Van Der Perre, "Massive MIMO for 5G," *IEEE 5G Tech Focus*, vol. 1, no. 11, pp. 1–4, Mar. 2017.

[16] T. L. Marzetta, "Massive MIMO: An introduction," *Bell Labs Tech. J.*, vol. 20, pp. 11–22, Mar. 2015.

[17] X. Ge, S. Tu, G. Mao, T. Han, and C. X. Wang, "5G ultra-dense cellular networks," *IEEE Trans. Wireless Commun.*, vol. 23, no. 1, pp. 72–79, Feb. 2016.

[18] R. Zhang, C. Qi, Y. Li, Y. Ruan, C.-X. Wang, and H. Zhang, "Towards energy-efficient underlaid device-to-device communications: A joint resource management approach," *IEEE Access*, vol. 7, pp. 31385–31396, 2019.

[19] D. Liu, Y. Chen, K. K. Chai, T. Zhang, and M. Elkashlan, "Two-dimensional optimization on user association and green energy allocation for HetNets with hybrid energy sources," *IEEE Trans. Commun.*, vol. 63, no. 11, pp. 4111–4124, Nov. 2015.

[20] L. A. Fletscher, J. M. Maestre, and C. V. Peroni, "Coalitional planning for energy efficiency of HetNets powered by hybrid energy sources," *IEEE Trans. Veh. Technol.*, vol. 67, no. 7, pp. 6573–6584, Jul. 2018.

[21] L. A. Fletscher, J. Barreiro-Gomez, C. Ocampo-Martinez, C. V. Peroni, and J. M. Maestre, "Atomicity and non-anonymity in population-like games for the energy efficiency of hybrid-power HetNets," *IEEE Trans. Netw. Service Manage.*, vol. 15, no. 4, pp. 1600–1614, Dec. 2018.

[22] B. Rengarajan, G. Rizzo, and M. A. Marsan, "Energy-optimal base station density in cellular access networks with sleep modes," *Comput. Netw.*, vol. 78, pp. 152–163, Feb. 2015.

[23] M. Di Renzo, A. Zappone, T. T. Lam, and M. Debbah, "System-level modeling and optimization of the energy efficiency in cellular networks—A stochastic geometry framework," *IEEE Trans. Wireless Commun.*, vol. 17, no. 4, pp. 2539–2556, Apr. 2018.

[24] I. Keshavarzian, Z. Zeinalpour-Yazdi, and A. Tadaion, "Energy-efficient mobility-aware caching algorithms for clustered small cells in ultra-dense networks," *IEEE Trans. Veh. Technol.*, vol. 68, no. 7, pp. 6833–6846, Jul. 2019.

[25] P. Munoz, R. Barco, and S. Fortes, "Conflict resolution between load balancing and handover optimization in LTE networks," *IEEE Commun. Lett.*, vol. 18, no. 10, pp. 1795–1798, Oct. 2014.

[26] K. Haneda *et al.*, "Indoor 5G 3GPP-like channel models for office and shopping mall environments," in *Proc. IEEE Int. Conf. Commun. Workshops (ICC)*, Kuala Lumpur, Malaysia, May 2016, pp. 694–699.

[27] K. Haneda *et al.*, "5G 3GPP-like channel models for outdoor urban microcellular and macrocellular environments," in *Proc. IEEE 83rd Veh. Technol. Conf. (VTC Spring)*, Nanjing, China, May 2016, pp. 1–7.

[28] G. R. MacCartney and T. S. Rappaport, "Rural macrocell path loss models for millimeter wave wireless communications," *IEEE J. Sel. Areas Commun.*, vol. 35, no. 7, pp. 1663–1677, Jul. 2017.

[29] H. Jiang, D. Tang, J. Zhou, X. Xi, J. Feng, J. Dang, and L. Wu, "Approximation algorithm based channel estimation for massive MIMO antenna array systems," *IEEE Access*, vol. 7, pp. 149364–149372, 2019.

[30] J. R. Perez and R. P. Torres, "On the impact of the radiation pattern of the antenna element on MU-MIMO indoor channels," *IEEE Access*, vol. 8, pp. 25459–25467, 2020.

[31] A. Al-Wahhamy, H. Al-Rizzo, and N. E. Buris, "Efficient evaluation of massive MIMO channel capacity," *IEEE Syst. J.*, vol. 14, no. 1, pp. 614–620, Mar. 2020.

[32] T. L. Marzetta, E. G. Larsson, H. Yang, and H. Q. Ngo, *Fundamentals of Massive MIMO*. Cambridge, U.K.: Cambridge Univ. Press, 2018.

[33] E. Bjornson and E. G. Larsson, "How energy-efficient can a wireless communication system become?" in *Proc. 52nd Asilomar Conf. Signals, Syst., Comput.*, Pacific Grove, CA, USA, Oct. 2018, pp. 1252–1256.

[34] M. Masoudi *et al.*, "Green mobile networks for 5G and beyond," *IEEE Access*, vol. 7, pp. 107270–107299, 2019.

[35] Z. Dong, J. Wei, X. Chen, and P. Zheng, "Energy efficiency optimization and resource allocation of cross-layer broadband wireless communication system," *IEEE Access*, vol. 8, pp. 50740–50754, 2020.

[36] K. M. S. Huq, S. Mumtaz, J. Bachmatiuk, J. Rodriguez, X. Wang, and R. L. Aguiar, "Green HetNet CoMP: Energy efficiency analysis and optimization," *IEEE Trans. Veh. Technol.*, vol. 64, no. 10, pp. 4670–4683, Oct. 2015.

[37] G. Auer, V. Giannini, C. Desset, I. Godor, P. Skillermark, M. Olsson, M. Imran, D. Sabella, M. Gonzalez, O. Blume, and A. Fehske, "How much energy is needed to run a wireless network?" *IEEE Wireless Commun.*, vol. 18, no. 5, pp. 40–49, Oct. 2011.

[38] J. Carmona-Murillo, I. Soto, F. J. Rodríguez-Pérez, D. Cortés-Polo, and J. L. González-Sánchez, "Performance evaluation of distributed mobility management protocols: Limitations and solutions for future mobile networks," *Mobile Inf. Syst.*, vol. 2017, pp. 1–15, Feb. 2017.
[39] E. M. O. Fafolahan and S. Pierre, "A seamless mobility management protocol in 5G locator identificator split dense small cells," *IEEE Trans. Mobile Comput.*, vol. 19, no. 8, pp. 1745–1759, Aug. 2020.
[40] D. Shin, K. Yun, J. Kim, P. V. Astillo, J.-N. Kim, and I. You, "A security protocol for route optimization in DMM-based smart home IoT networks," *IEEE Access*, vol. 7, pp. 142531–142550, 2019.
[41] J. Kim, P. V. Astillo, and I. You, "DMM-SEP: Secure and efficient protocol for distributed mobility management based on 5G networks," *IEEE Access*, vol. 8, pp. 76028–76042, 2020.
[42] C. A. C. Coello, G. B. Lamont, D. A. V. Veldhuizen, *Evolutionary Algorithms for Solving Multi-Objective Problems*, 2nd ed. New York, NY, USA: Springer, 2007.
[43] C. Blum and A. Roli, "Metaheuristics in combinatorial optimization: Overview and conceptual comparison," *ACM Comput. Surv.*, vol. 35, no. 3, pp. 268–308, Sep. 2003.
[44] E. Zitzler and L. Thiele, "Multiobjective evolutionary algorithms: A comparative case study and the strength Pareto approach," *IEEE Trans. Evol. Comput.*, vol. 3, no. 4, pp. 257–271, Nov. 1999.
[45] K. Deb, A. Pratap, S. Agarwal, and T. Meyarivan, "A fast and elitist multiobjective genetic algorithm: NSGA-II," *IEEE Trans. Evol. Comput.*, vol. 6, no. 2, pp. 182–197, Apr. 2002.
[46] A. J. Nebro, J. J. Durillo, J. Garcia-Nieto, C. A. Coello Coello, F. Luna, and E. Alba, "SMPSO: A new PSO-based Metaheuristic for multi-objective optimization," in *Proc. IEEE Symp. Comput. Intell. Milti-Criteria Decis.-Making*, Nashville, TN, USA, Mar. 2009, pp. 66–73.
[47] S. García, D. Molina, M. Lozano, and F. Herrera, "A study on the use of non-parametric tests for analyzing the evolutionary algorithms' behaviour: A case study on the CEC'2005 special session on real parameter optimization," *J. Heuristics*, vol. 15, no. 6, pp. 617–644, Dec. 2009.
[48] J. Knowles, "A summary-attainment-surface plotting method for visualizing the performance of stochastic multiobjective optimizers," in *Proc. 5th Int. Conf. Intell. Syst. Design Appl. (ISDA)*, Warsaw, Poland, Sep. 2005, pp. 552–557.

ALEJANDRO RAMÍREZ-ARROYO was born in Córdoba, Spain, in 1997. He received the B.Sc. degree in telecommunication engineering from the Universidad de Granada, Spain, in 2019, where he is currently pursuing the M.Sc. degree in telecommunication engineering. His current research interests include heterogeneous networks, optimization techniques, and propagation channels and models for 5G networks.

PABLO H. ZAPATA-CANO received the B.Sc. degree in telecommunications engineering from the Universidad de Granada, Spain. He is currently a SMARTNET M.Sc. Scholar with TelecomSud Paris, where he was a recipient of an Erasmus Mundus grant. Since 2018, he has been also active in research as a Graduate Research Assistant with the Universidad de Granada, publishing several articles in international journals and conferences. His research interests include wireless communications, 5G Ultradense networks, green communications, and optimization techniques.

ÁNGEL PALOMARES-CABALLERO was born in Jaen, Spain, in 1994. He received the B.Sc. and M.Sc. degrees in telecommunication engineering from the Universidad de Granada (UGR), Spain, in 2016 and 2018, respectively. He is currently pursuing the Ph.D. degree with a national predoctoral fellowship. Since 2017, he has been with the Department of Signal Theory, Telematics and Communications, Universidad de Granada. His research interests include millimeter-wave antennas and phase shifters, gap-waveguide, structures with higher symmetries, and optimization algorithms.

JAVIER CARMONA-MURILLO (Member, IEEE) received the Ph.D. degree in computer science and communications from the University of Extremadura, Spain, in 2015. From 2005 to 2009, he was a Research and Teaching Assistant. Since 2009, he has been an Associate Professor with the Department of Computing and Telematics System Engineering, Universidad de Extremadura. During the past years, he has spent research periods with the Centre for Telecommunications Research, King's College London, U.K., and Aarhus University, Denmark. His current research interests include 5G networks, mobility management protocols, performance evaluation, and the quality of service support in future mobile networks.

FRANCISCO LUNA-VALERO (Associate Member, IEEE) received the degree in engineering and the Ph.D. degree in computer science from the University of Málaga, Spain, in 2002 and 2008, respectively. Until 2012, he was a Research Assistant with the University of Málaga. In 2012, he held a postdoctoral position the Universidad Carlos III of Madrid. In 2013, he was with the Universidad de Extremadura as an Assistant Professor. Since 2015, he has been an Associate Professor with the University of Málaga. His current research interests include the design and implementation of parallel and multi-objective meta-heuristics, and their application to solve complex problems arising in several domains, including telecommunications, finance, and structural design.

JUAN F. VALENZUELA-VALDÉS was born in Marbella, Spain. He received the degree in telecommunications engineering from the Universidad de Málaga, Spain, in 2003, and the Ph.D. degree from the Universidad Politécnica de Cartagena, Spain, in May 2008. In 2004, he joined the Department of Information Technologies and Communications, Universidad Politécnica de Cartagena. In 2007, he joined the Head of research with EMITE Ing. In 2011, he joined the Universidad de Extremadura, and in 2015, he joined the Universidad de Granada, where he is currently an Associate Professor. He was a Co-Founder of Emite Ing., a spin-off company. He also holds several national and international patents. His publication record is composed of more than 80 publications, including 40 JCR indexed articles, more than 30 contributions in international conferences and 7 book chapter. His current research interests include wireless communications and efficiency in wireless sensor networks. He has also been awarded several prizes, including a National Prize to the Best Ph.D. in mobile communications by Vodafone and the i-patentes award by the Spanish Autonomous Region of Murcia for innovation and technology transfer excellence.